Electronic Supplementary Material (ESI) for Materials Chemistry Frontiers.
This journal is © the Partner Organisations 2019

Supporting Information:

Enhanced intrinsic saturation magnetization of $Zn_xCo_{1-x}Fe_2O_4$ nanocrystallites with metastable spinel inversion†

Henrik Lyder Andersen,[a] Cecilia Granados-Miralles,‡[a] Matilde Saura-Múzquiz,[a] Marian Stingaciu,⁑[a] Jacob Larsen,[b] Frederik Søndergaard-Pedersen,[a] Jakob Voldum Ahlburg,[a] Lukas Keller,[c] Cathrine Frandsen[b] and Mogens Christensen*[a]

[a]Center for Materials Crystallography, Department of Chemistry and Interdisciplinary Nanoscience Centre (iNANO), Aarhus University, DK-8000 Aarhus C, Denmark
[b]Department of Physics, Technical University of Denmark, DK-2800 Kgs. Lyngby, Denmark
[c]Laboratory for Neutron Scattering and Imaging, Paul Scherrer Institut, 5232 Villigen, Switzerland
‡Current address: Instituto de Cerámica y Vidrio, Consejo Superior de Investigaciones Científicas (CSIC), Kelsen 5, 28049 Madrid, Spain
⁑Current address: Institute for Energy Technology, IFE Neutron Material Characterisation, Instituttveien 18, NO-2007 Kjeller, Norway
*E-mail: mch@chem.au.dk

Table of Contents

Saturation magnetization of $Zn_xCo_{1-x}Fe_2O_4$ in the literature **2**
Powder diffraction data **3**
Magnetic structure model 3
Refinement R-values 4
Rietveld refinements (x=0.0-0.3, As-synthesized) 5
Rietveld refinements (x=0.4-0.7, As-synthesized) 6
Rietveld refinements (x=0.8-1.0, As-synthesized) 7
Rietveld refinements (x=0.0-0.3, Annealed) 8
Rietveld refinements (x=0.4-1.0, Annealed) 9
Peak sharpening and hematite impurity 10
Transmission electron microscopy images **11**
TEM (x=0.2, As-synthesized) 11
TEM (x=0.4, As-synthesized) 12
TEM (x=0.8, As-synthesized) 13
TEM (x=0.2, Annealed) 14
TEM (x=0.4, Annealed) 15
TEM (x=0.8, Annealed) 16
Scanning transmission electron microscopy and energy dispersive X-ray spectroscopy data **17**
STEM-EDS quantitative analysis summary 17
STEM-EDS maps + spectrum (x=0.2, As-synthesized) 18
STEM-EDS maps + spectrum (x=0.4, As-synthesized) 19
STEM-EDS maps + spectrum (x=0.8, As-synthesized) 20
STEM-EDS maps + spectrum (x=0.2, Annealed) 21
STEM-EDS maps + spectrum (x=0.4, Annealed) 22
STEM-EDS maps + spectrum (x=0.8, Annealed) 23
Vibrating sample magnetometry data **24**
Hysteresis curves (x=0.0-1.0, As-synthesized) 24
Hysteresis curves (x=0.0-1.0, Annealed) 25
Coercive field and magnetic remanence 26
References **27**

Saturation magnetization of $Zn_xCo_{1-x}Fe_2O_4$ in the literature

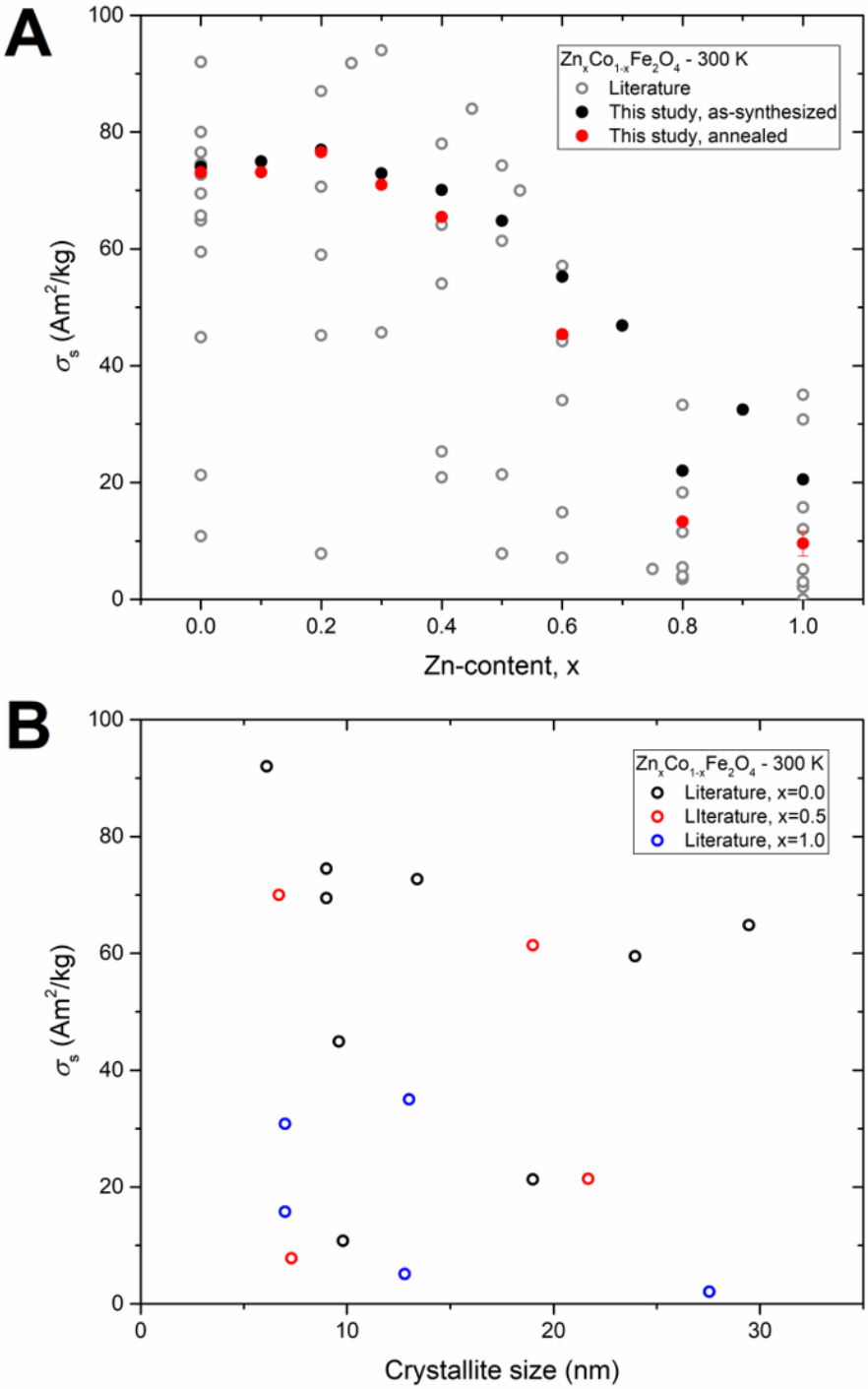

Figure S1: A) Room-temperature mass-specific saturation magnetizations, σ_s, of $Zn_xCo_{1-x}Fe_2O_4$ nanocrystallites as function of Zn-content. Literature values are shown in grey and values from this study in black (as-synthesized) and red (annealed) dots. B) Literature values for room-temperature mass specific saturation magnetizations as function of crystallite size for selected compositions, *i.e.* x=0.0 (black), x=0.5 (red) and x=1.0 (blue).[1-10]

Powder diffraction data

Magnetic structure model

The magnetic structure was implemented as an additional phase of the type "Magnetic Phase" with lowest symmetry space group of the corresponding centering, *i.e. F*-1. The special positions of the magnetic species (Fe^{3+} and Co^{2+} on the tetrahedral and octahedral sites) were specified, from which all magnetic spins were generated by providing the first 24 symmetry operations (see ESI†) of the *Fd*-3*m* space group and considering the centrosymmetry.

```
F -1                <--Space group symbol for hkl generation
!Nsym Cen Laue MagMat
  24   2   1   1
!
SYMM x,y,z
MSYM u,v,w, 0.000
SYMM -x+3/4,-y+1/4,z+1/2
MSYM u,v,w, 0.000
SYMM -x+1/4,y+1/2,-z+3/4
MSYM u,v,w, 0.000
SYMM x+1/2,-y+3/4,-z+1/4
MSYM u,v,w, 0.000
SYMM z,x,y
MSYM u,v,w, 0.000
SYMM z+1/2,-x+3/4,-y+1/4
MSYM u,v,w, 0.000
SYMM -z+3/4,-x+1/4,y+1/2
MSYM u,v,w, 0.000
SYMM -z+1/4,x+1/2,-y+3/4
MSYM u,v,w, 0.000
SYMM y,z,x
MSYM u,v,w, 0.000
SYMM -y+1/4,z+1/2,-x+3/4
MSYM u,v,w, 0.000
SYMM y+1/2,-z+3/4,-x+1/4
MSYM u,v,w, 0.000
SYMM -y+3/4,-z+1/4,x+1/2
MSYM u,v,w, 0.000
SYMM y+3/4,x+1/4,-z+1/2
MSYM u,v,w, 0.000
SYMM -y,-x,-z
MSYM u,v,w, 0.000
SYMM y+1/4,-x+1/2,z+3/4
MSYM u,v,w, 0.000
SYMM -y+1/2,x+3/4,z+1/4
MSYM u,v,w, 0.000
SYMM x+3/4,z+1/4,-y+1/2
MSYM u,v,w, 0.000
SYMM -x+1/2,z+3/4,y+1/4
MSYM u,v,w, 0.000
SYMM -x,-z,-y
MSYM u,v,w, 0.000
```

SYMM x+1/4,-z+1/2,y+3/4
MSYM u,v,w, 0.000
SYMM z+3/4,y+1/4,-x+1/2
MSYM u,v,w, 0.000
SYMM z+1/4,-y+1/2,x+3/4
MSYM u,v,w, 0.000
SYMM -z+1/2,y+3/4,x+1/4
MSYM u,v,w, 0.000
SYMM -z,-y,-x
MSYM u,v,w, 0.000

Refinement R-values

Table S1: Summary of R-values from the combined structural refinement of the PXRD and NPD data.

	PXRD			NPD			
Zn-content, x	R_{wp} (%)	R_{Bragg} (%)	R_F (%)	R_{wp} (%)	R_{Bragg} (%)	R_F (%)	R_{magn} (%)
As-synthesized							
0.0	11.7	9.11	9.57	6.04	1.42	1.27	0.722
0.1	9.75	3.38	3.21	5.17	0.861	0.688	0.627
0.2	10.9	5.49	6.36	6.22	1.90	1.29	0.675
0.3	10.5	3.60	3.41	7.62	1.07	0.896	1.35
0.4	11.0	5.99	5.85	7.14	1.77	1.14	1.93
0.5	10.3	5.27	4.95	7.70	1.80	1.39	2.53
0.6	10.3	4.87	4.46	7.93	1.91	1.38	3.86
0.7	10.3	2.16	2.06	10.7	2.04	1.60	3.19
0.8	10.7	3.00	2.75	8.59	2.60	1.56	5.40
0.9	10.3	2.41	2.05	9.90	1.44	1.40	3.92
1.0	11.8	4.23	3.49	7.82	2.40	1.74	5.17
Annealed							
0.0	4.12	3.53	3.56	5.25	1.96	1.34	1.77
0.1	5.58	4.80	4.14	5.99	1.95	0.874	1.33
0.2	4.87	4.59	4.11	10.8	4.26	2.98	4.05
0.3	5.75	4.45	3.87	6.47	1.66	1.02	2.16
0.4	5.60	3.78	3.38	9.22	3.95	2.42	6.01
0.6	4.95	4.50	4.38	11.7	4.74	2.93	12.1
0.8	5.24	3.89	3.99	12.9	3.51	2.47	9.76
1.0	4.69	1.83	2.62	6.45	1.49	1.35	4.67

Rietveld refinements (x=0.0-0.3, As-synthesized)

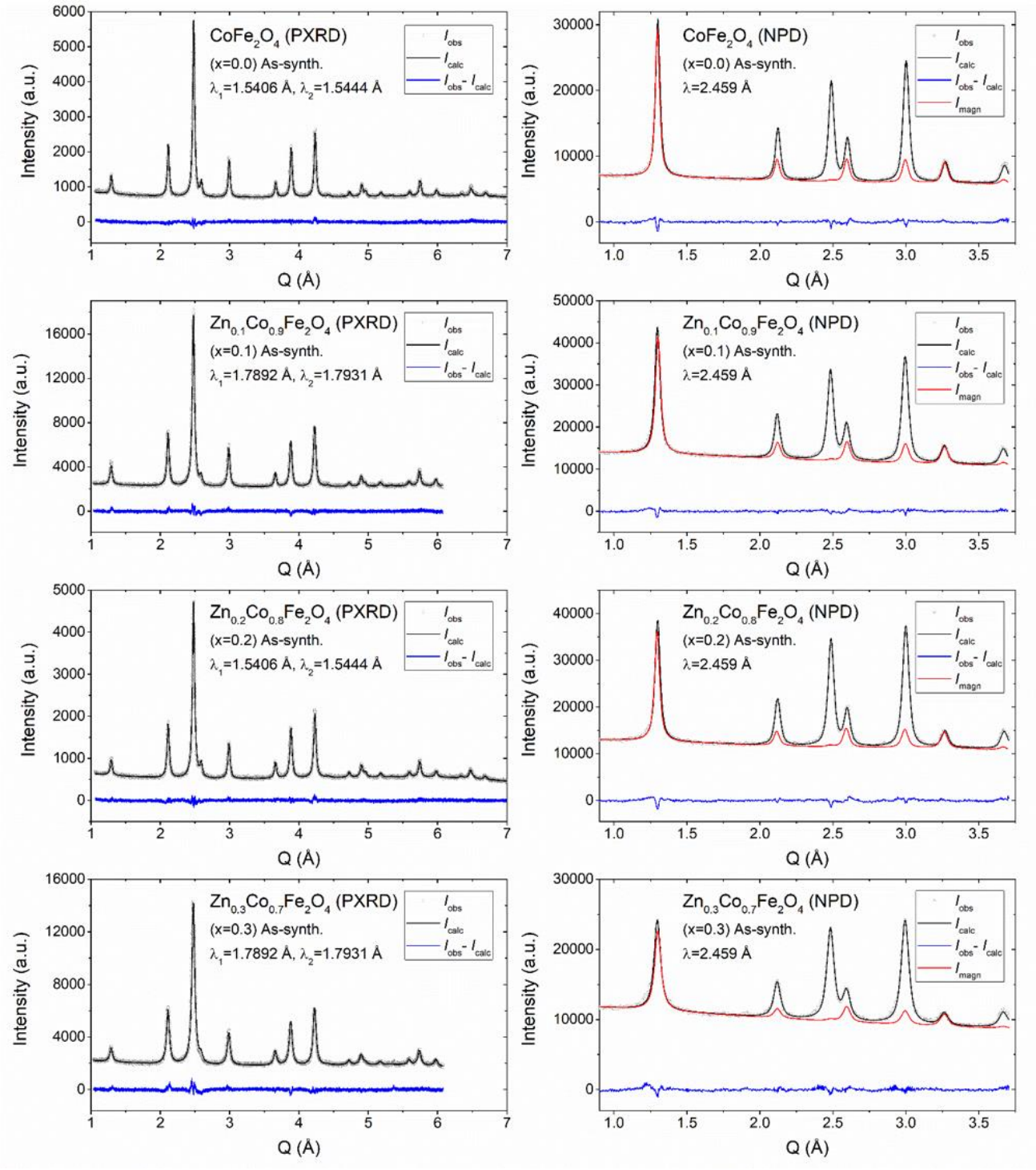

Figure S2: PXRD and NPD patterns of the indicated nanocrystalline samples and corresponding Rietveld fits obtained by combined refinement of a constrained structural model.

Rietveld refinements (x=0.4-0.7, As-synthesized)

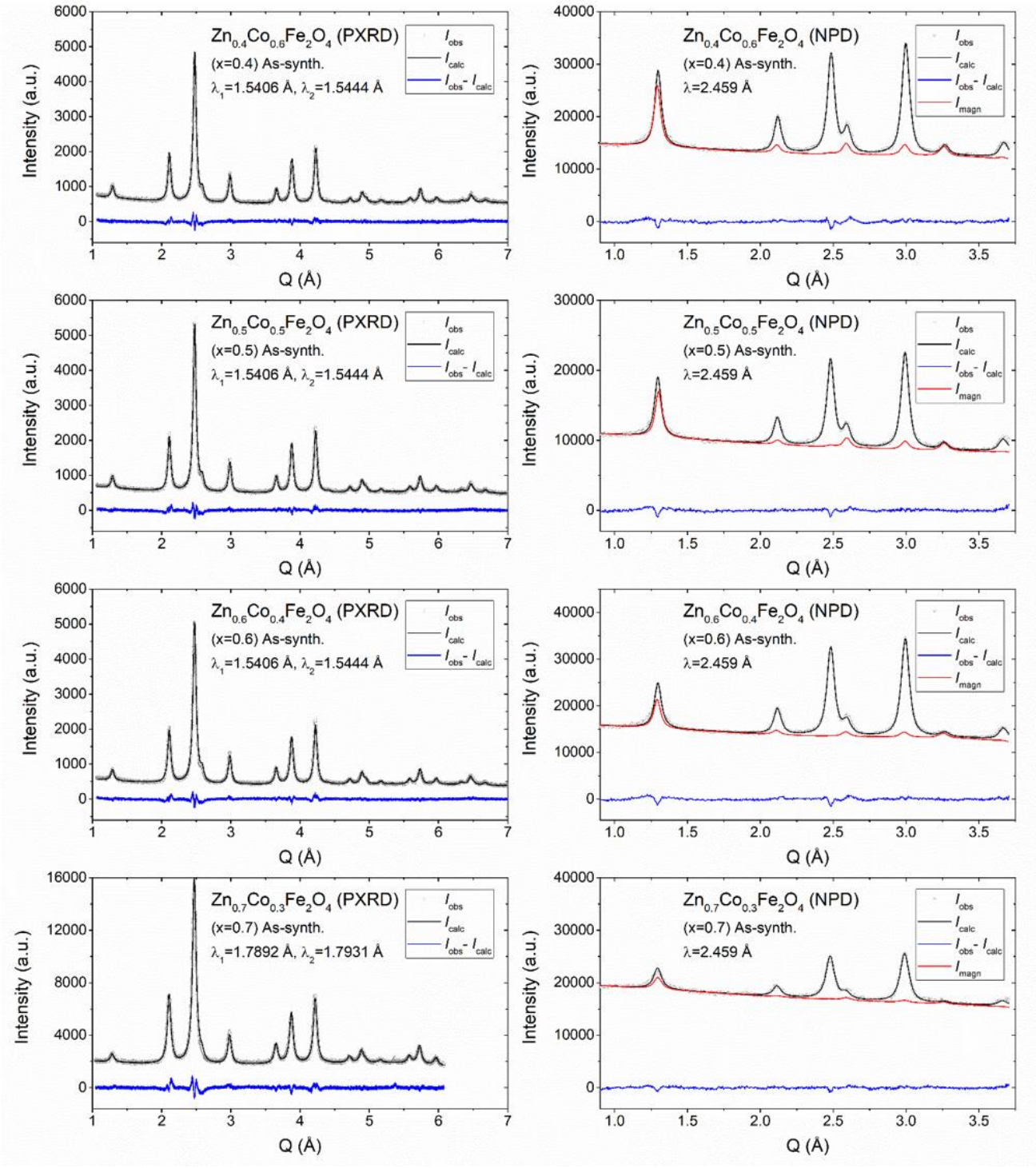

Figure S3: PXRD and NPD patterns of the indicated nanocrystalline samples and corresponding Rietveld fits obtained by combined refinement of a constrained structural model.

Rietveld refinements (x=0.8-1.0, As-synthesized)

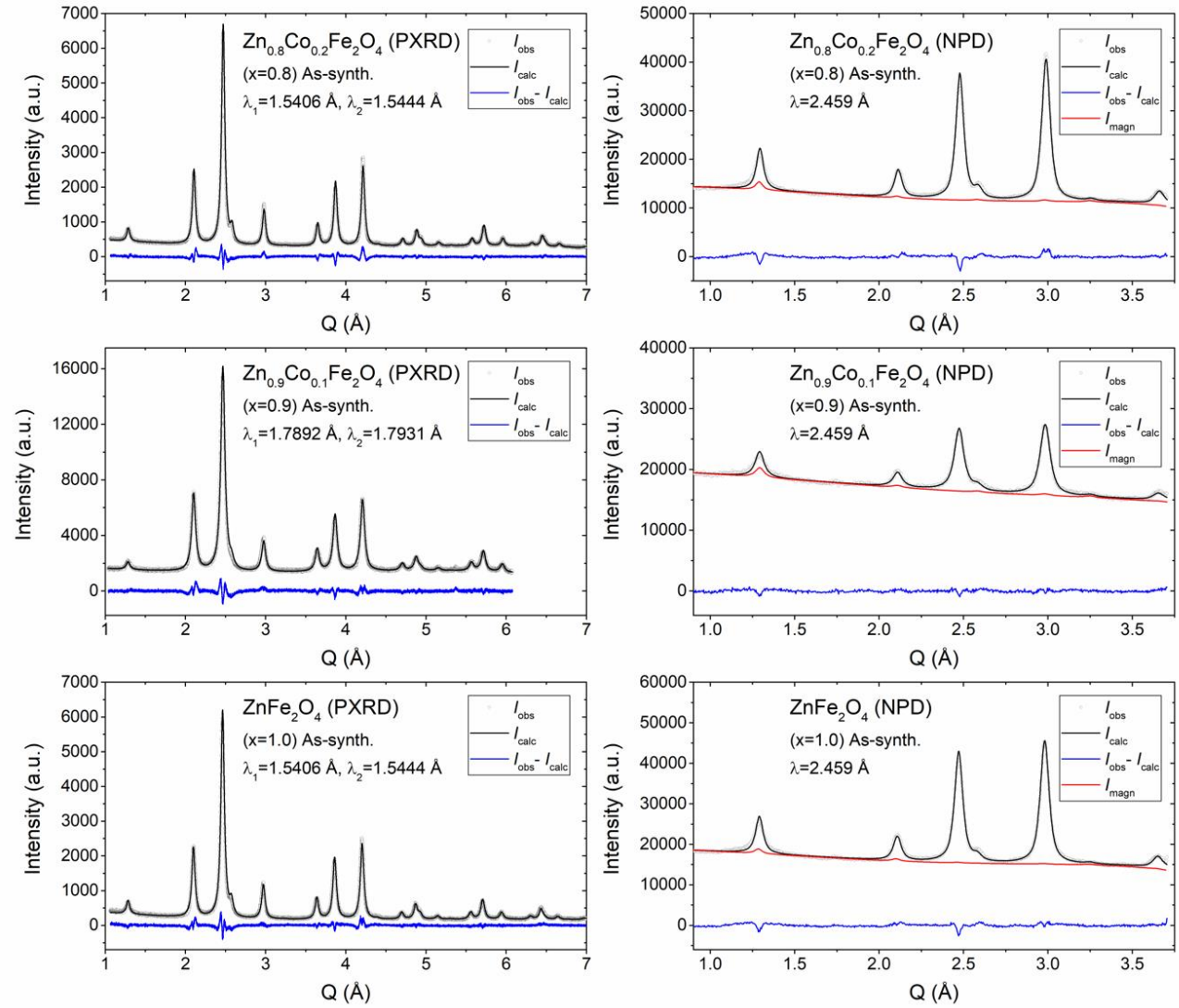

Figure S4: PXRD and NPD patterns of the indicated nanocrystalline samples and corresponding Rietveld fits obtained by combined refinement of a constrained structural model.

Rietveld refinements (x=0.0-0.3, Annealed)

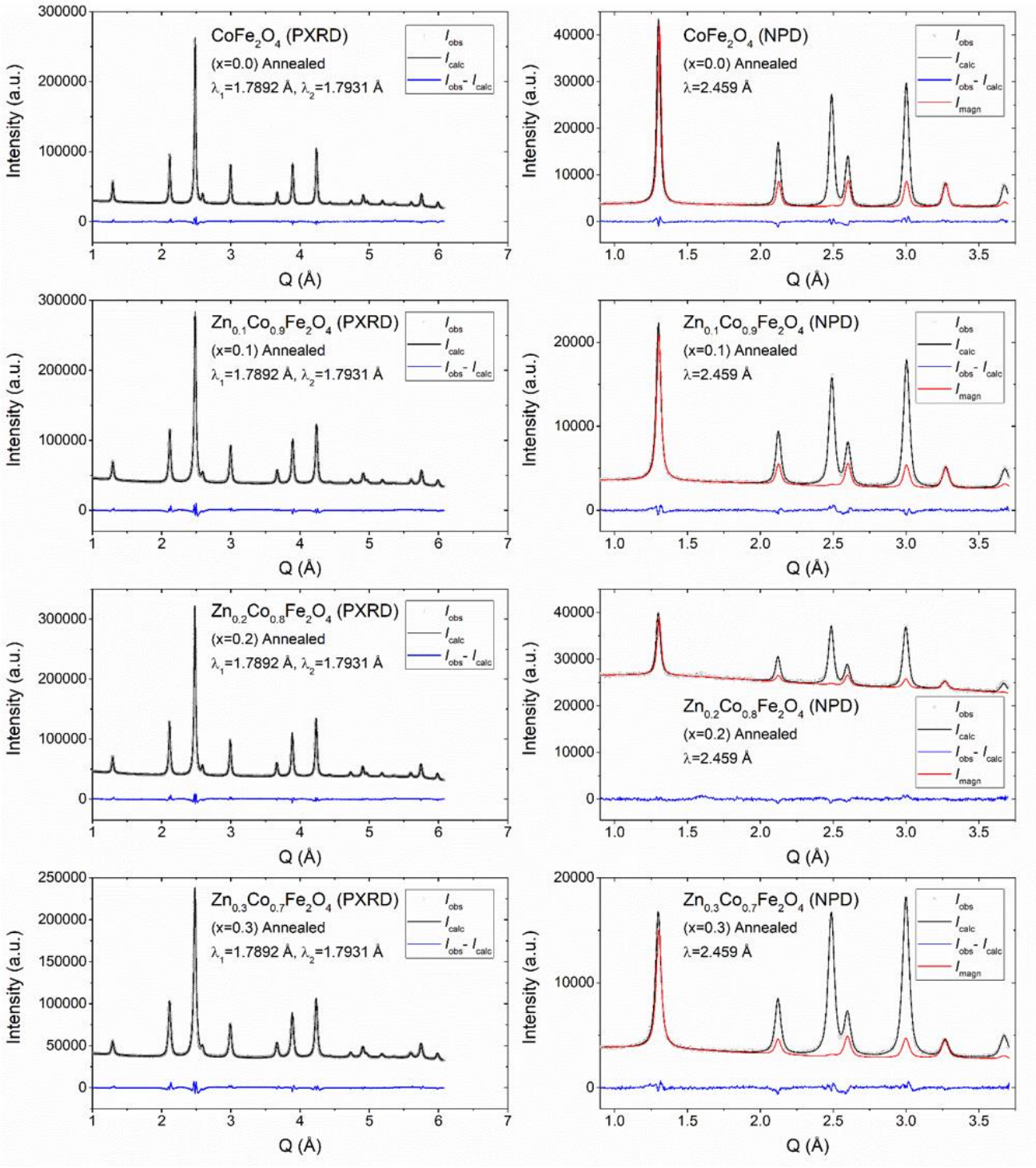

Figure S5: PXRD and NPD patterns of the indicated nanocrystalline samples and corresponding Rietveld fits obtained by combined refinement of a constrained structural model.

Rietveld refinements (x=0.4-1.0, Annealed)

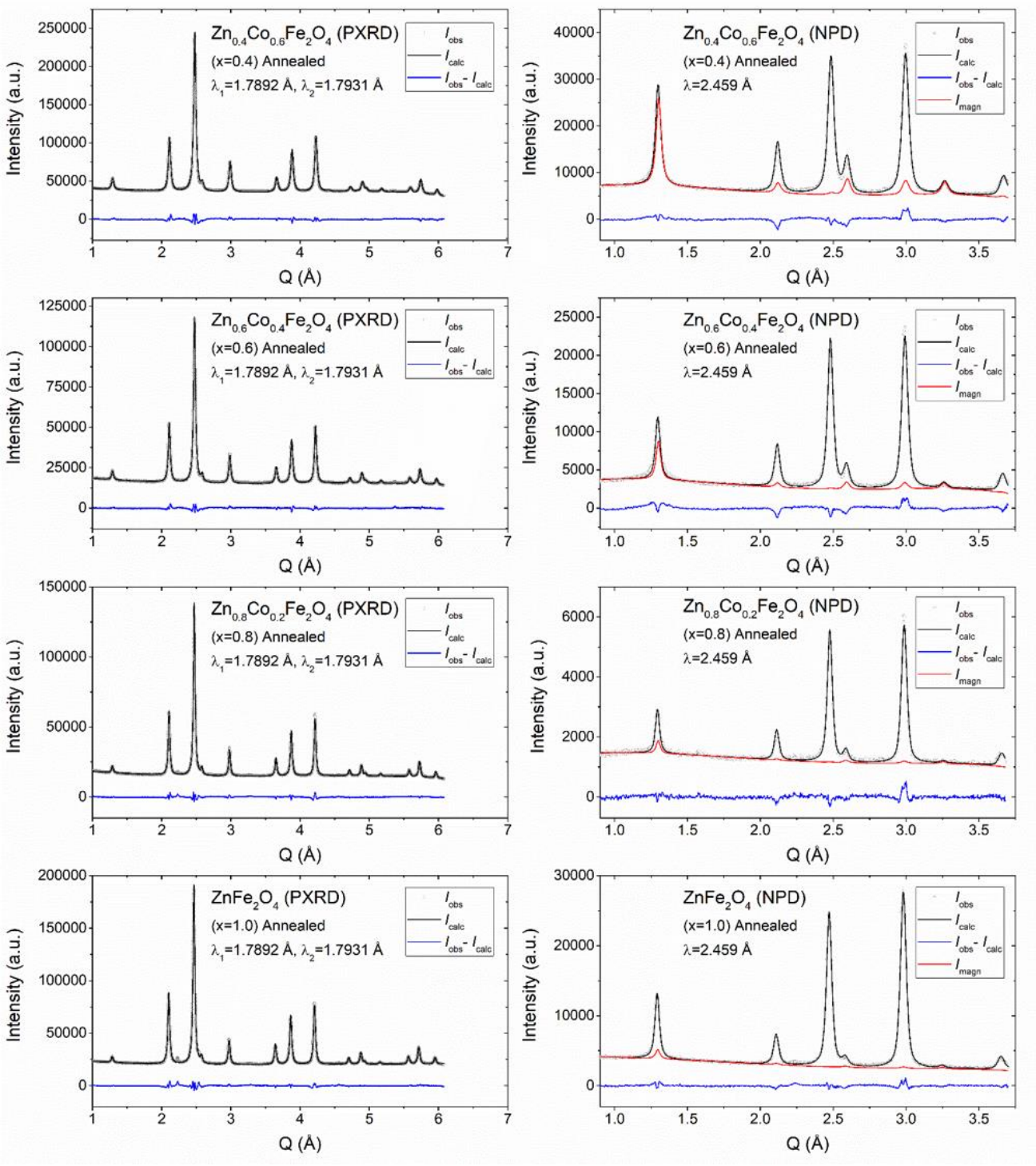

Figure S6: PXRD and NPD patterns of the indicated nanocrystalline samples and corresponding Rietveld fits obtained by combined refinement of a constrained structural model.

Peak sharpening and hematite impurity

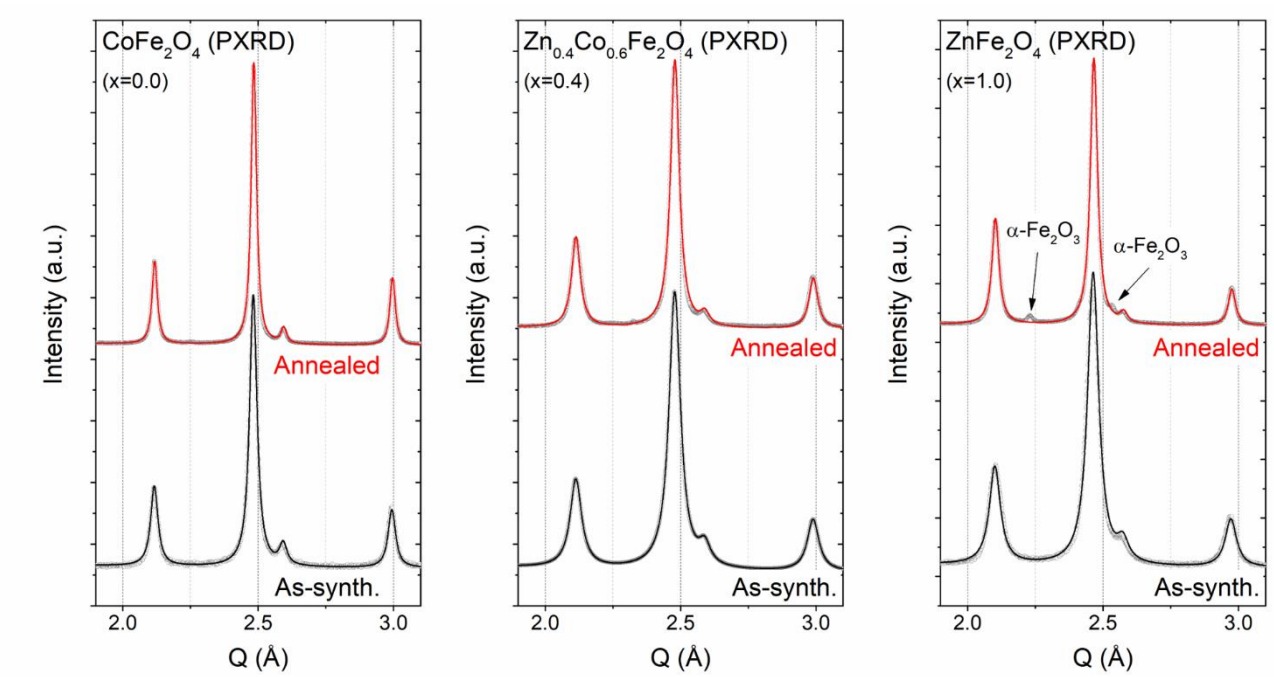

Figure S7: Enhancement of selected q-region of the PXRD data for the x=0.0, x=0.4 and x=1.0 samples before and after annealing illustrating the slight peak sharpening after annealing. The additional peaks arising from the presence of a small amount (<5%) of hematite (α-Fe_2O_3) in the x=1.0 sample are indicated in the figure.

Transmission electron microscopy images

TEM (x=0.2, As-synthesized)

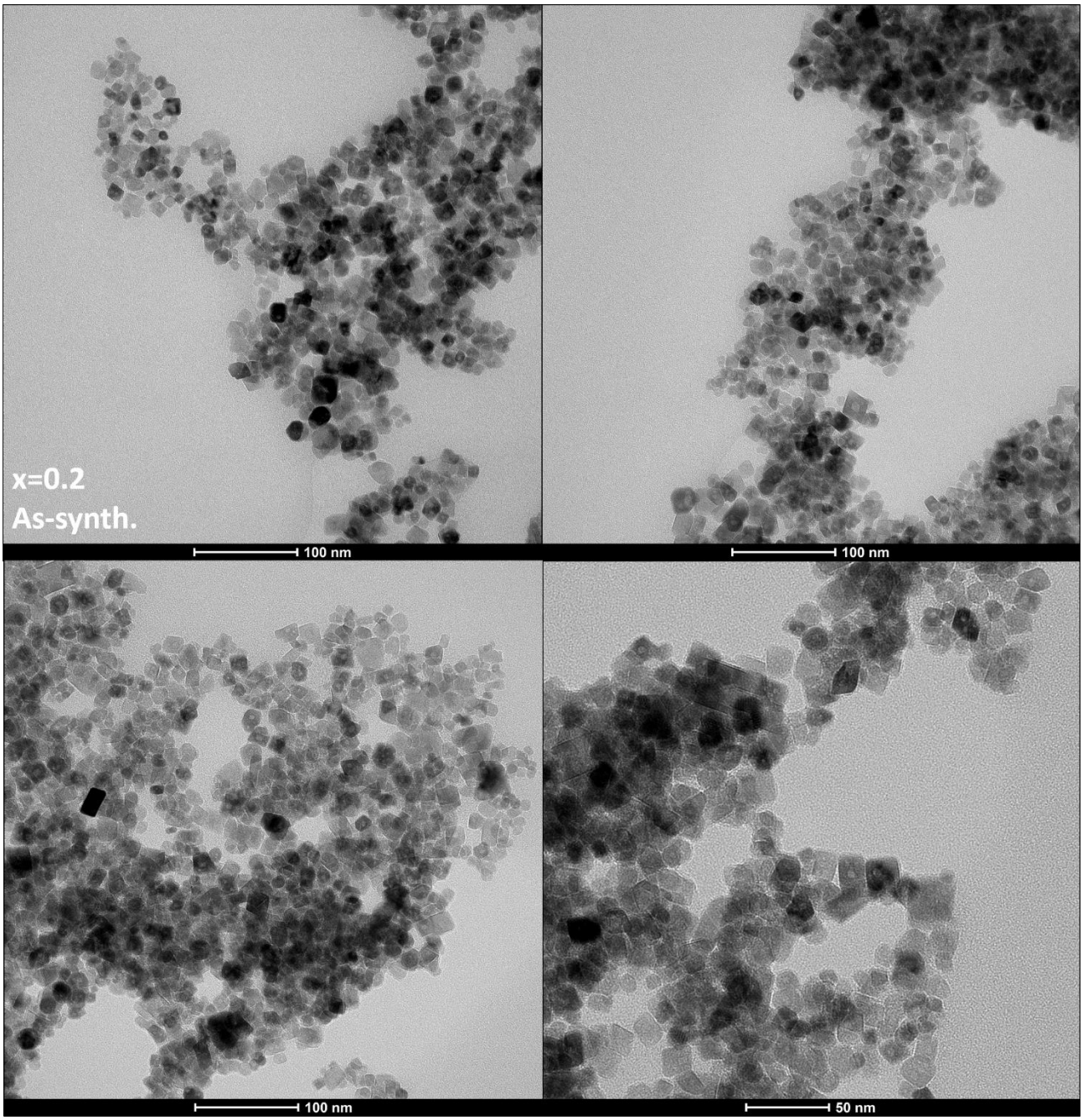

Figure S8: Additional TEM images of the as-synthesized $Zn_{0.2}Co_{0.8}Fe_2O_4$ (x=0.2) sample.

TEM (x=0.4, As-synthesized)

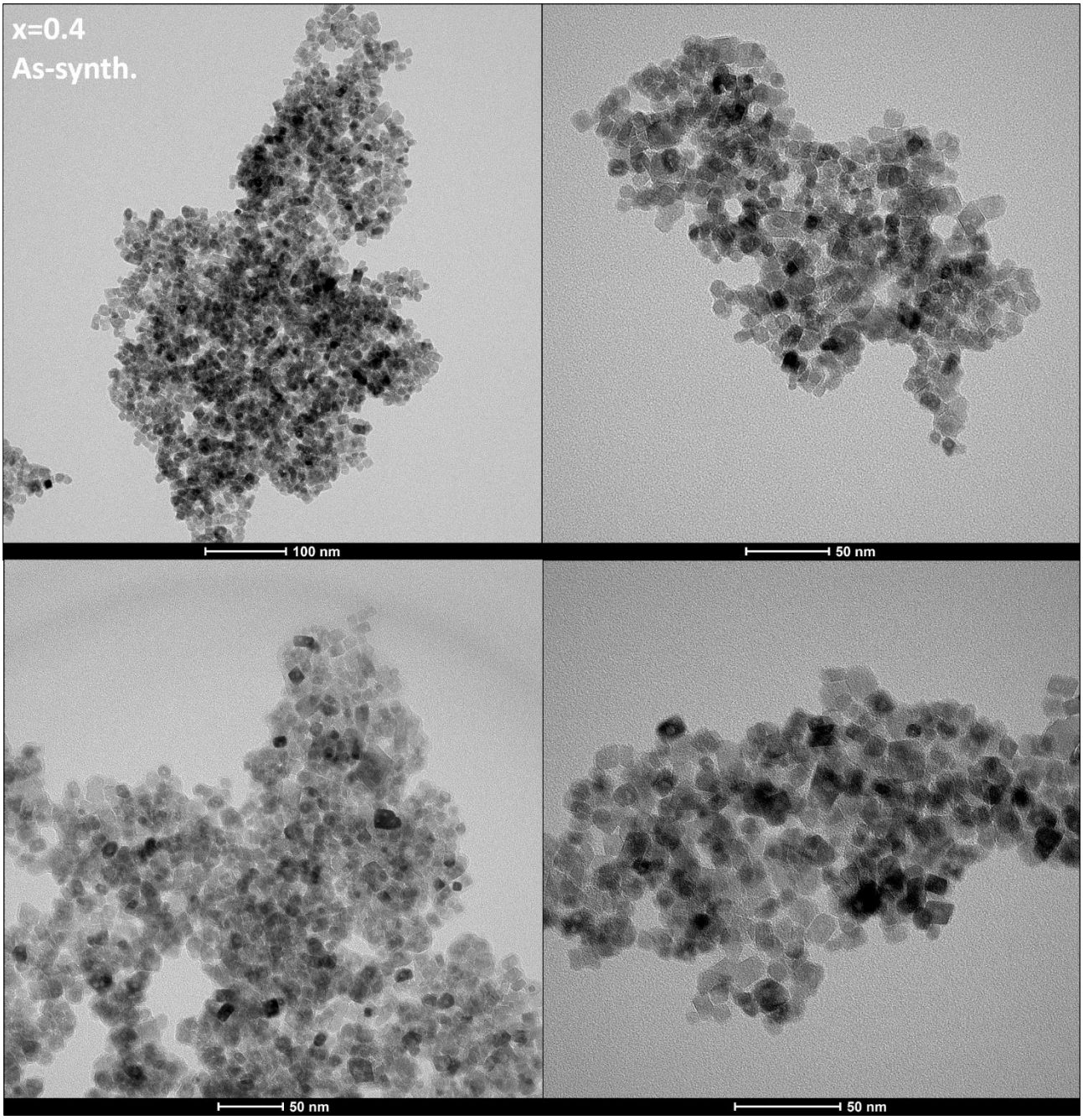

Figure S9: Additional TEM images of the as-synthesized $Zn_{0.4}Co_{0.6}Fe_2O_4$ (x=0.4) sample.

TEM (x=0.8, As-synthesized)

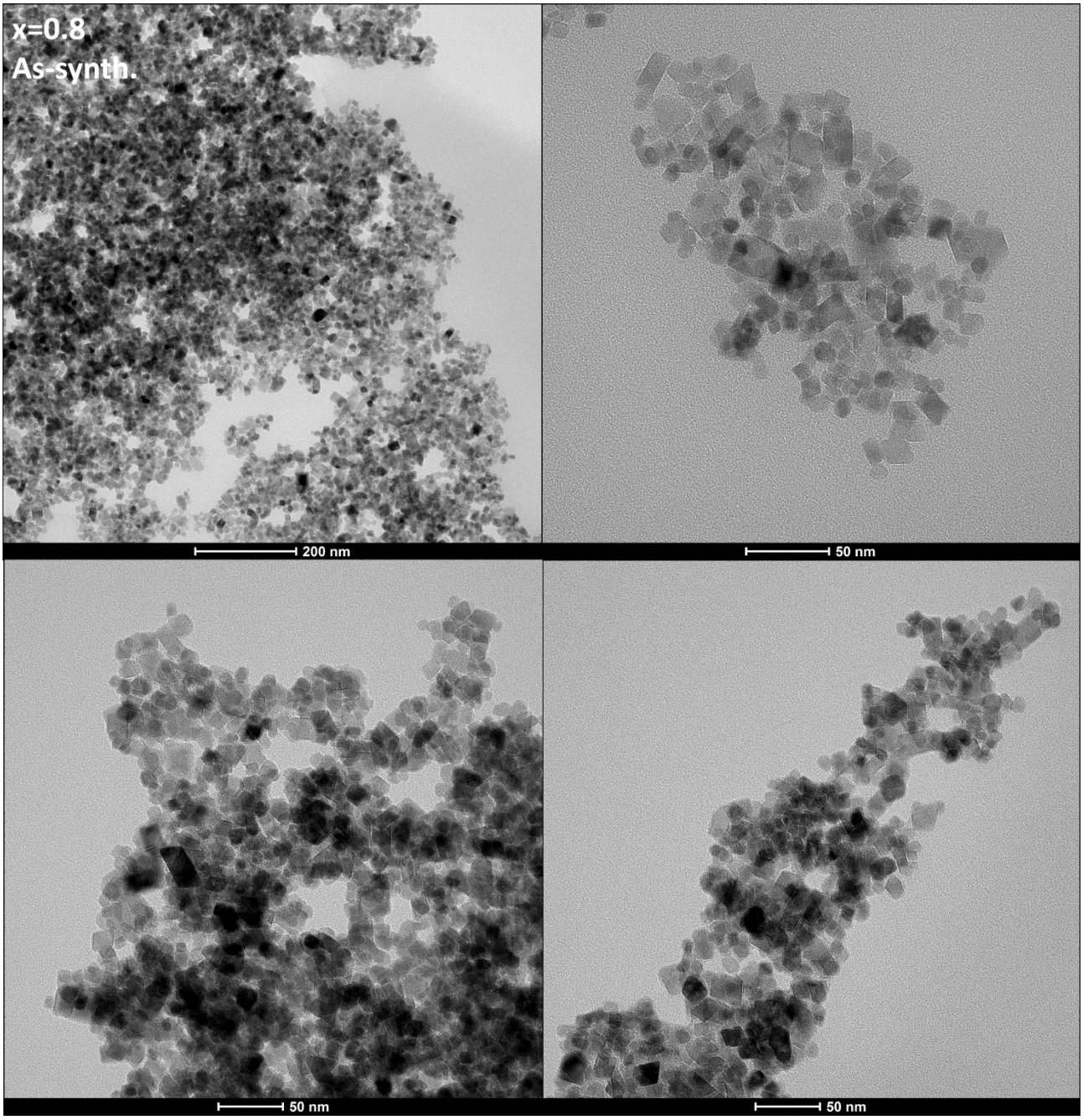

Figure S10: Additional TEM images of the as-synthesized $Zn_{0.8}Co_{0.2}Fe_2O_4$ (x=0.8) sample.

TEM (x=0.2, Annealed)

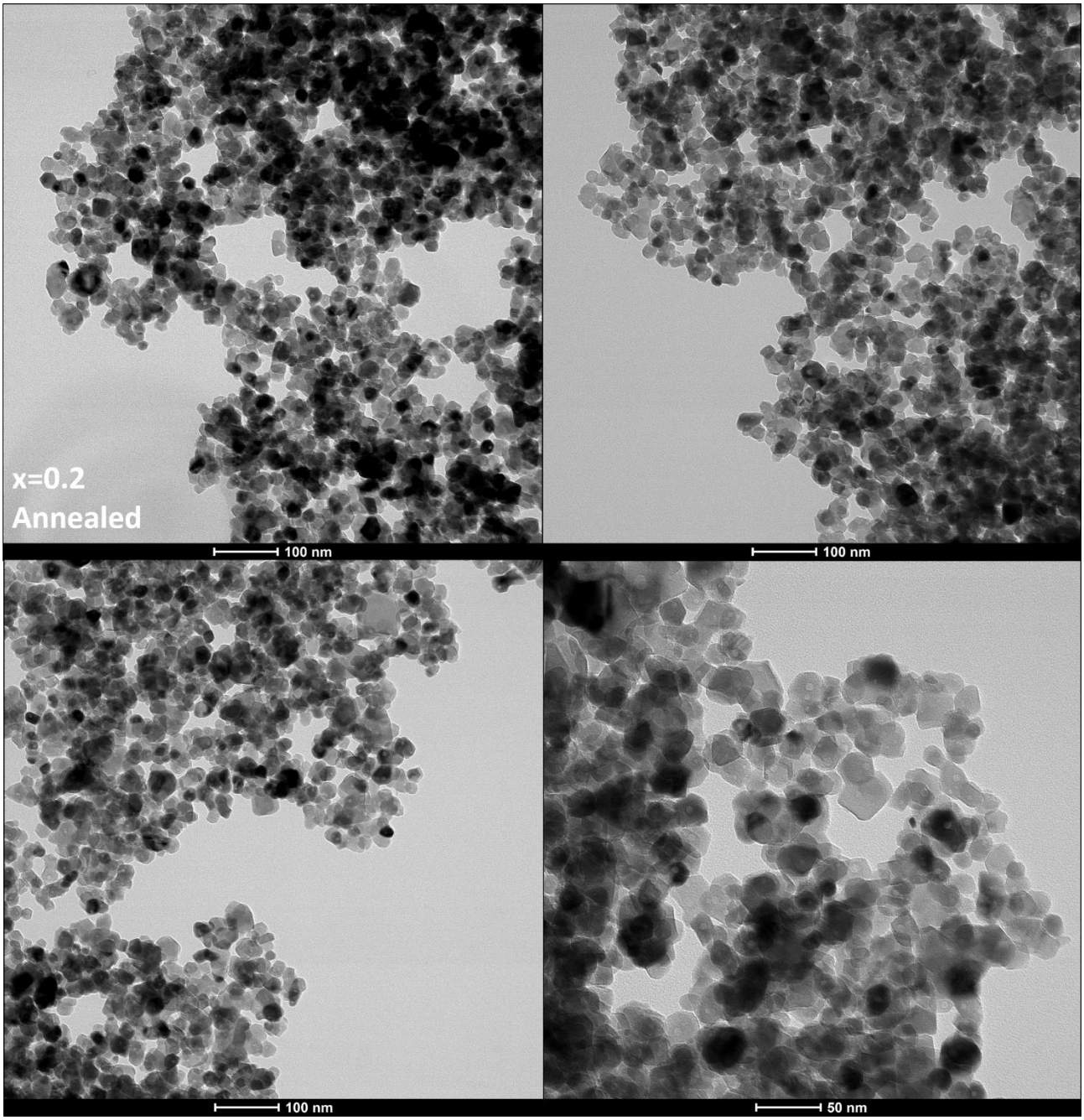

Figure S11: Additional TEM images of the annealed $Zn_{0.2}Co_{0.8}Fe_2O_4$ (x=0.2) sample.

TEM (x=0.4, Annealed)

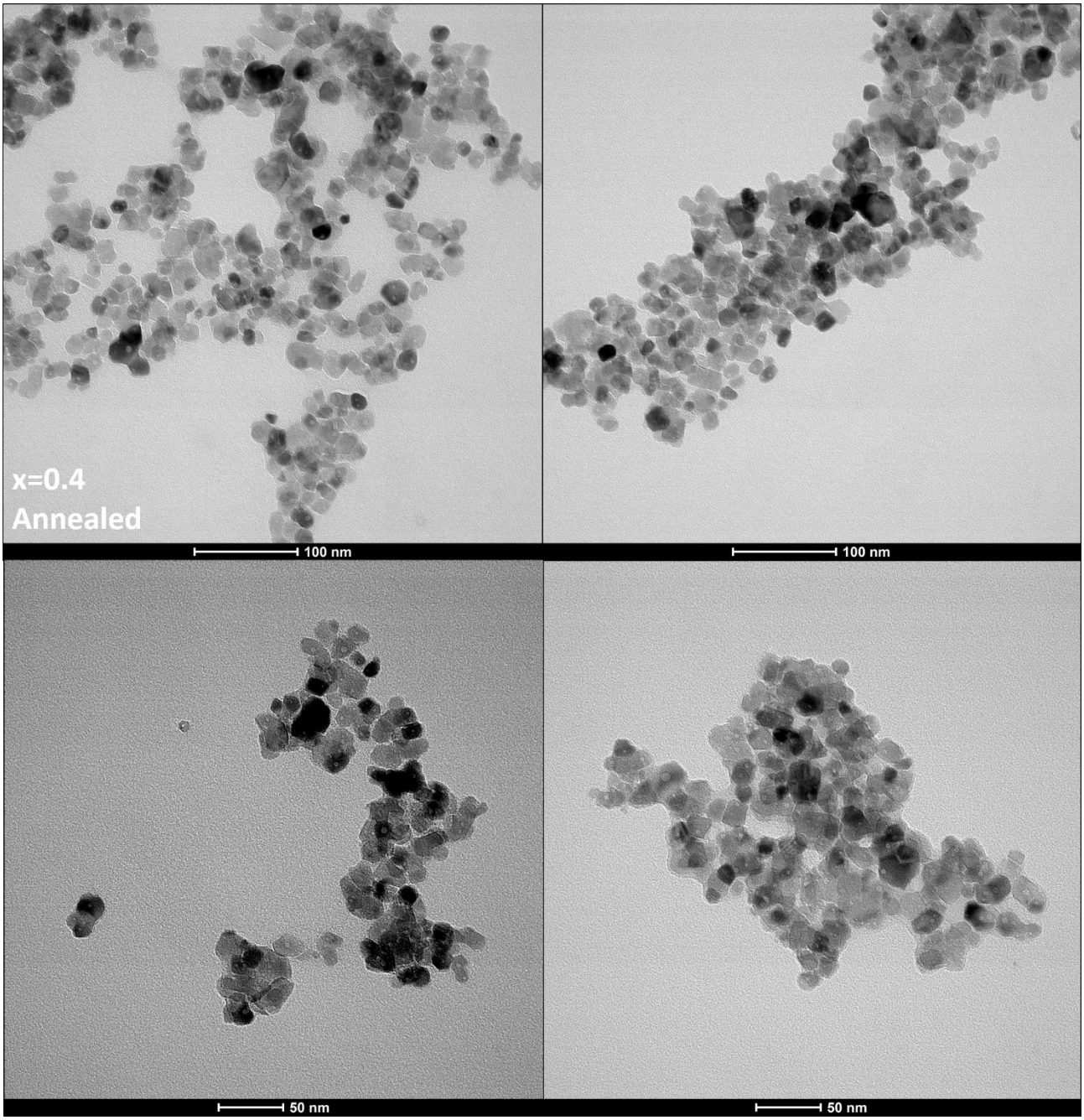

Figure S12: Additional TEM images of the annealed $Zn_{0.4}Co_{0.6}Fe_2O_4$ (x=0.4) sample.

TEM (x=0.8, Annealed)

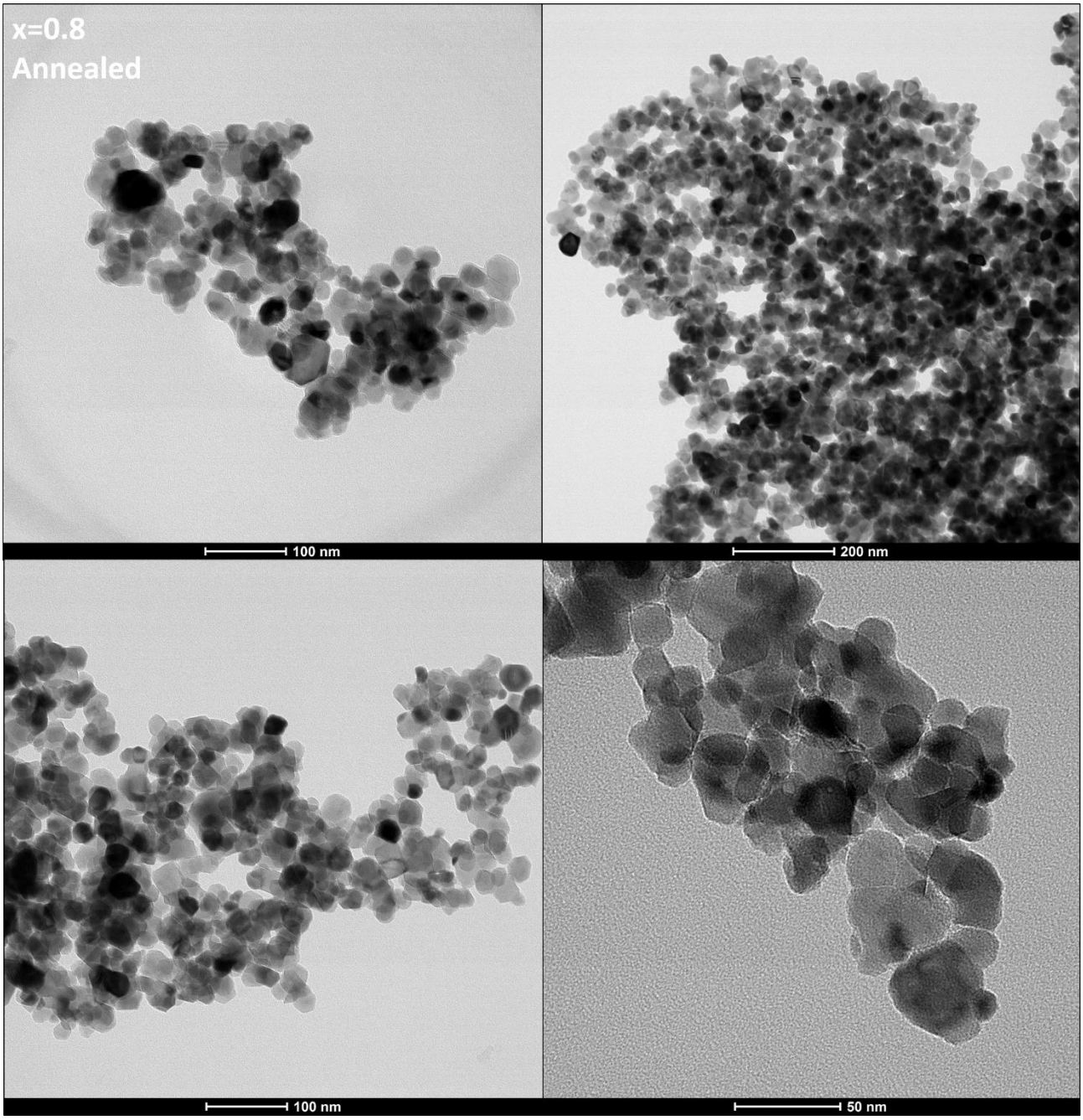

Figure S13: Additional TEM images of the annealed $Zn_{0.8}Co_{0.2}Fe_2O_4$ (x=0.8) sample.

Scanning transmission electron microscopy and energy dispersive X-ray spectroscopy data

STEM-EDS quantitative analysis summary

Table S2: Elemental atomic percentages (at%) and stoichiometry (x EDS) obtained from the quantitative analysis of the energy dispersive X-ray spectra.

x	Zn at% (%)	Co at% (%)	Fe at% (%)	O at% (%)	x EDS Zn^{2+}/M^{2+}
As-synthesized					
0.2	2.6(3)	10(1)	24(2)	64(6)	0.21(3)
0.4	4.0(4)	5.9(6)	19(2)	71(7)	0.40(5)
0.8	8.1(8)	1.9(3)	18(2)	72(7)	0.56(7)
Annealed					
0.2	2.6(3)	10(1)	24(2)	63(6)	0.20(3)
0.4	5.0(5)	6.8(7)	22(2)	66(6)	0.42(5)
0.8	8.1(8)	2.0(2)	18(2)	72(7)	0.80(10)

STEM-EDS maps + spectrum (x=0.2, As-synthesized)

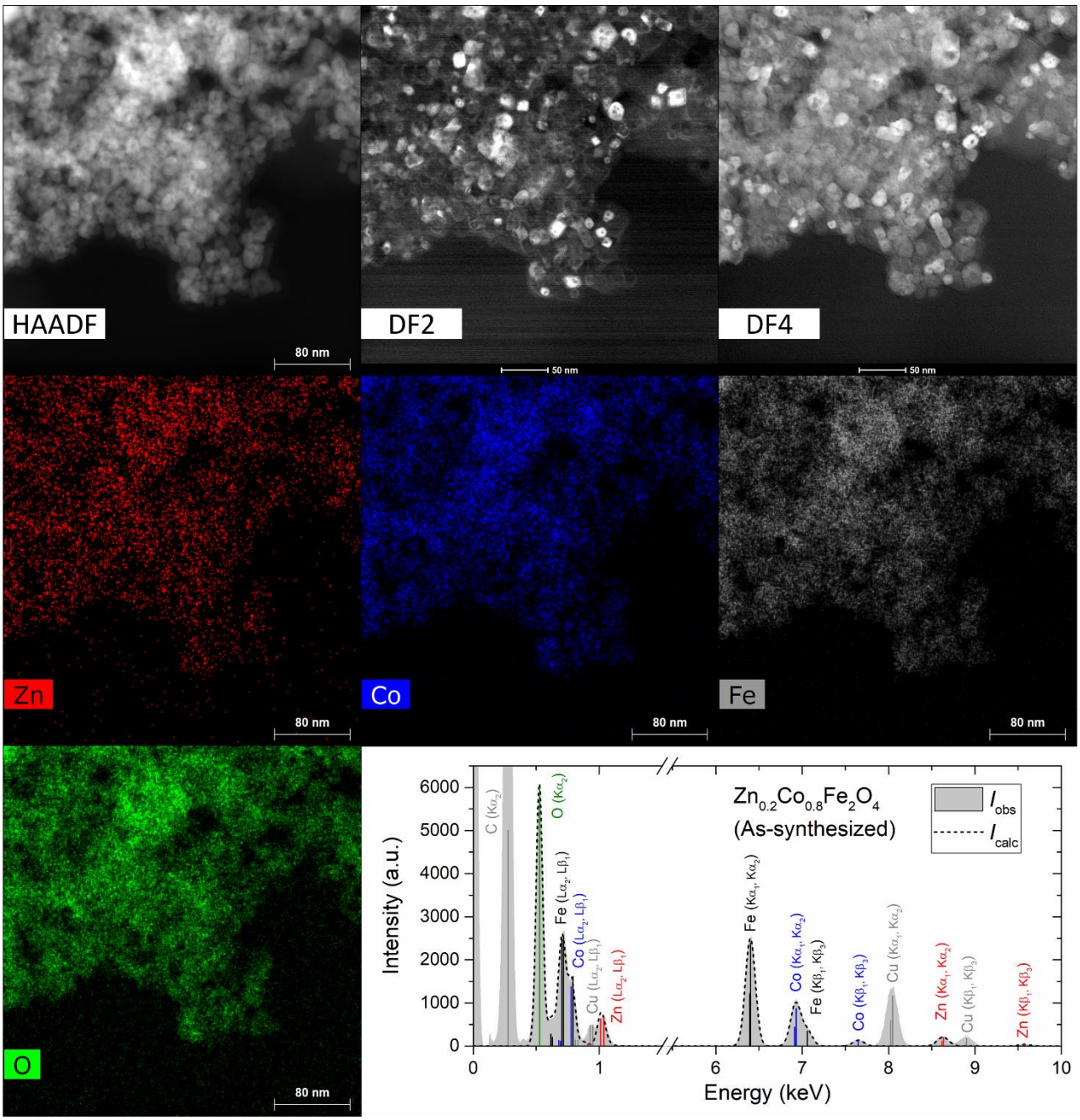

Figure S14: STEM-HAADF image, STEM-DF images and elemental maps illustrating the distribution of the constituent elements in the as-synthesized $Zn_{0.2}Co_{0.8}Fe_2O_4$ (x=0.2) sample. In the bottom right corner, the corresponding energy-dispersive X-ray spectrum from the region (gray area) and fit to the spectrum (dashed black line) is shown.

STEM-EDS maps + spectrum (x=0.4, As-synthesized)

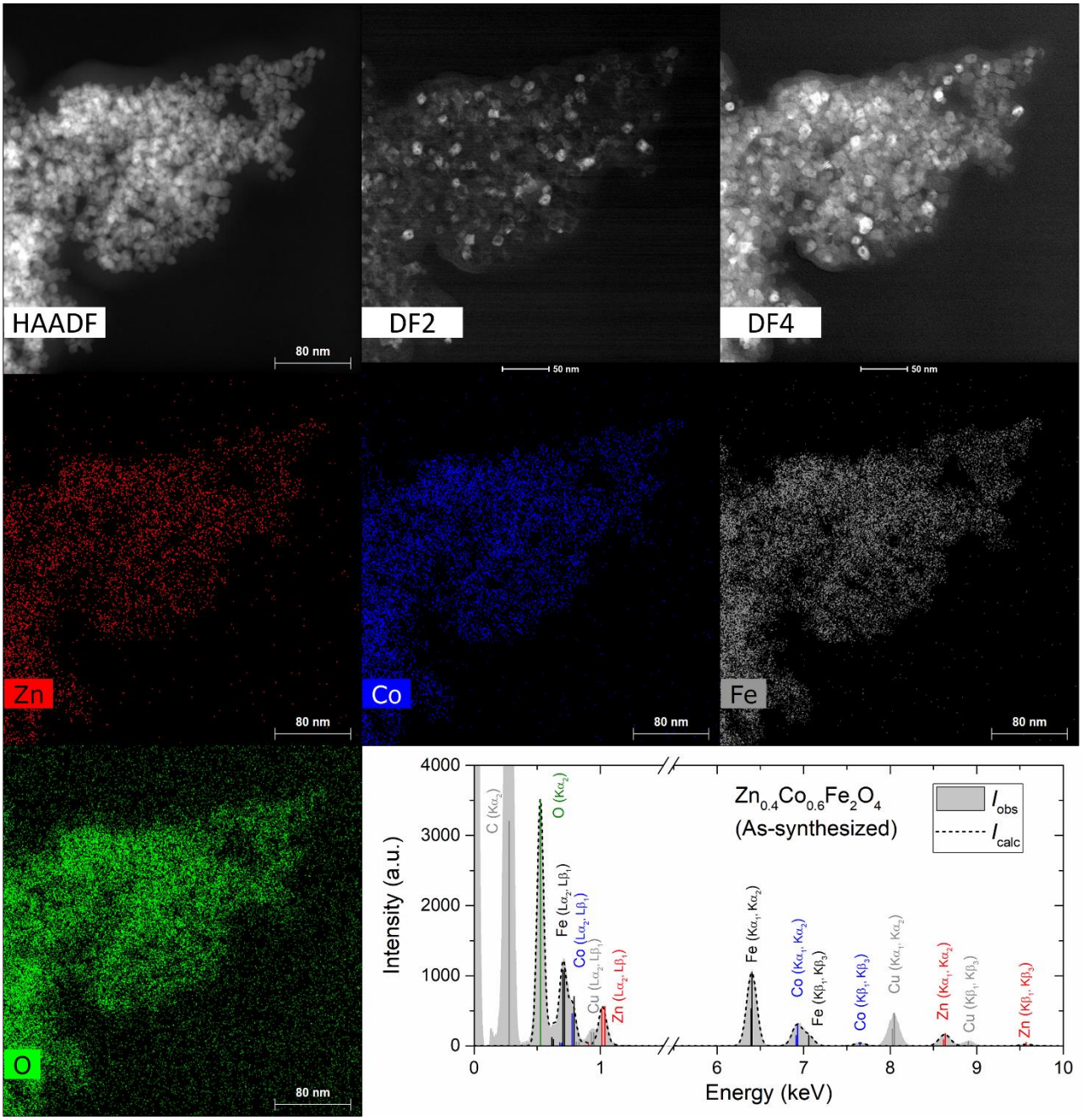

Figure S15: STEM-HAADF image, STEM-DF images and elemental maps illustrating the distribution of the constituent elements in the as-synthesized $Zn_{0.4}Co_{0.6}Fe_2O_4$ (x=0.4) sample. In the bottom right corner, the corresponding energy-dispersive X-ray spectrum from the region (gray area) and fit to the spectrum (dashed black line) is shown.

STEM-EDS maps + spectrum (x=0.8, As-synthesized)

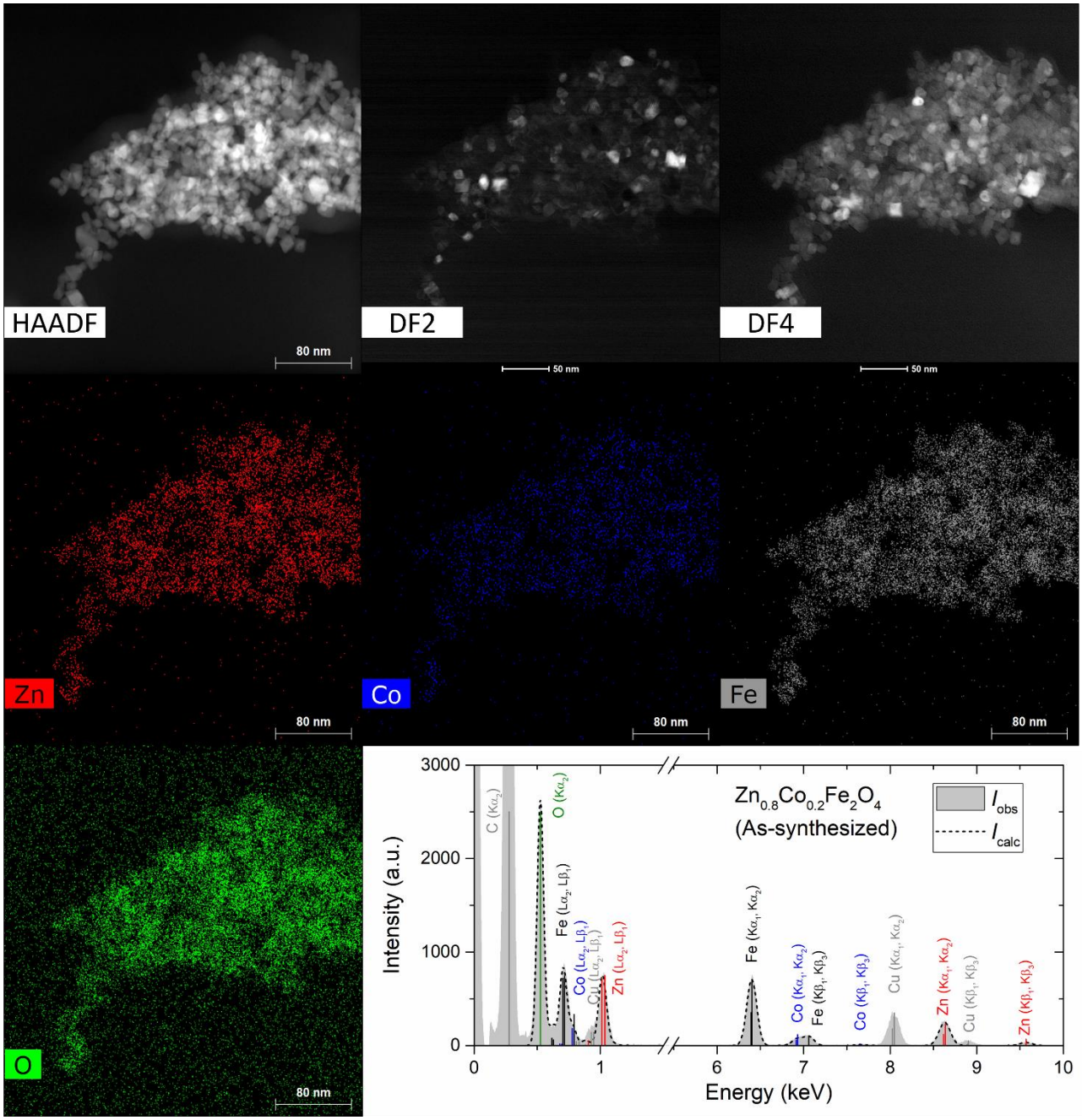

Figure S16: STEM-HAADF image, STEM-DF images and elemental maps illustrating the distribution of the constituent elements in the as-synthesized $Zn_{0.8}Co_{0.2}Fe_2O_4$ (x=0.8) sample. In the bottom right corner, the corresponding energy-dispersive X-ray spectrum from the region (gray area) and fit to the spectrum (dashed black line) is shown.

STEM-EDS maps + spectrum (x=0.2, Annealed)

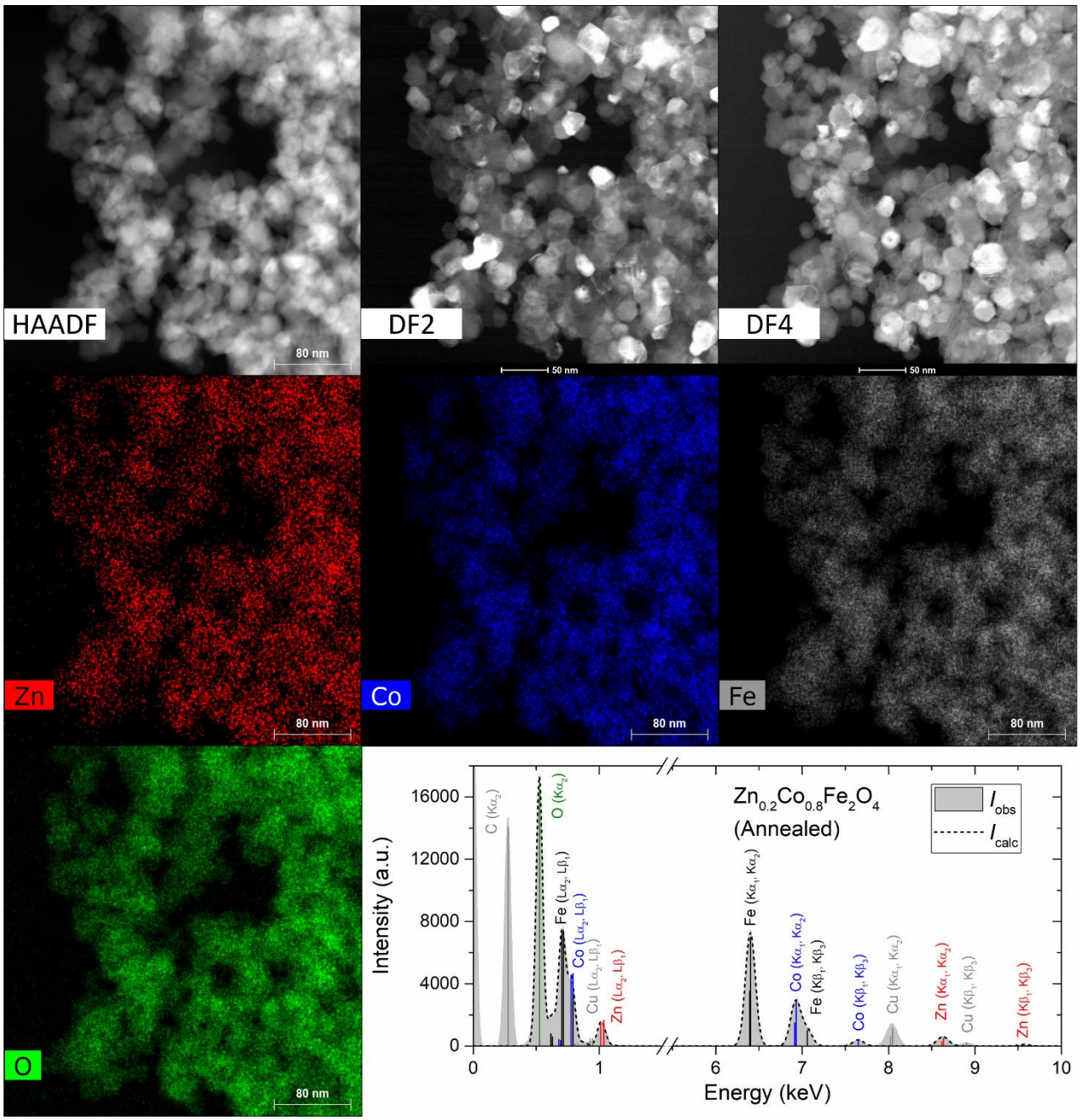

Figure S17: STEM-HAADF image, STEM-DF images and elemental maps illustrating the distribution of the constituent elements in the annealed $Zn_{0.2}Co_{0.8}Fe_2O_4$ (x=0.2) sample. In the bottom right corner, the corresponding energy-dispersive X-ray spectrum from the region (gray area) and fit to the spectrum (dashed black line) is shown.

STEM-EDS maps + spectrum (x=0.4, Annealed)

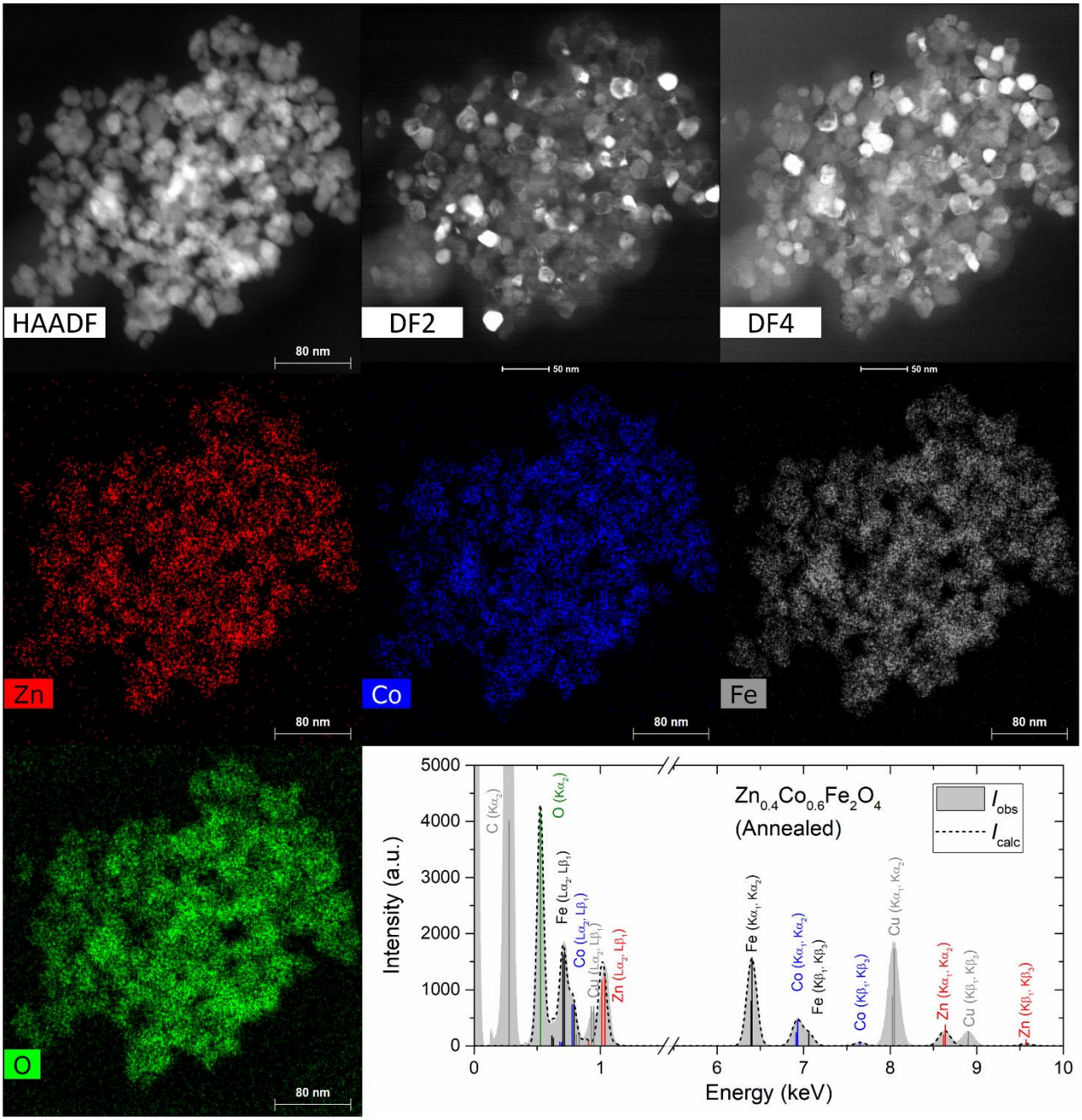

Figure S18: STEM-HAADF image, STEM-DF images and elemental maps illustrating the distribution of the constituent elements in the annealed $Zn_{0.4}Co_{0.6}Fe_2O_4$ (x=0.4) sample. In the bottom right corner, the corresponding energy-dispersive X-ray spectrum from the region (gray area) and fit to the spectrum (dashed black line) is shown.

STEM-EDS maps + spectrum (x=0.8, Annealed)

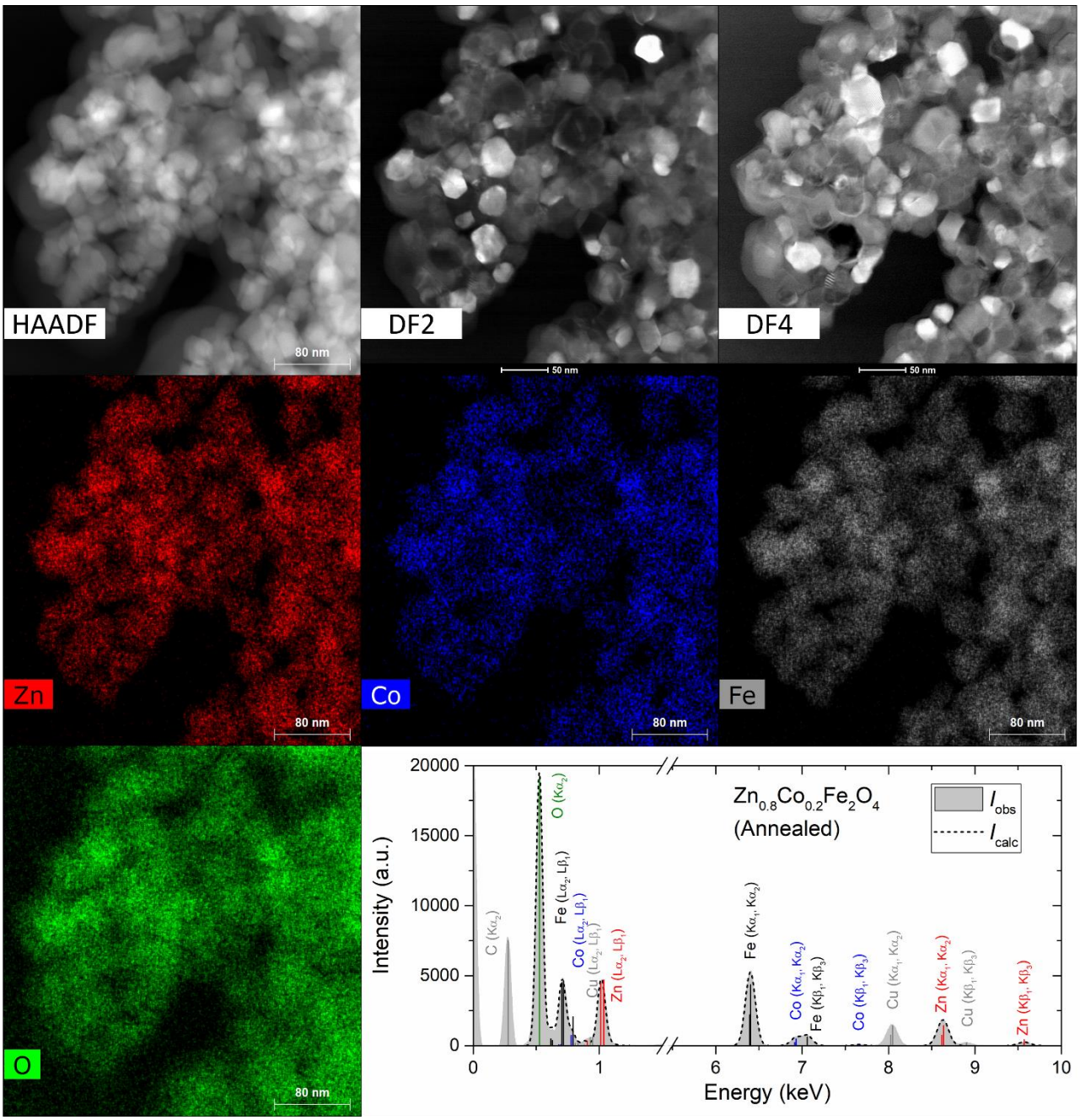

Figure S19: STEM-HAADF image, STEM-DF images and elemental maps illustrating the distribution of the constituent elements in the annealed $Zn_{0.8}Co_{0.2}Fe_2O_4$ (x=0.8) sample. In the bottom right corner, the corresponding energy-dispersive X-ray spectrum from the region (gray area) and fit to the spectrum (dashed black line) is shown.

Vibrating sample magnetometry data

Hysteresis curves (x=0.0-1.0, As-synthesized)

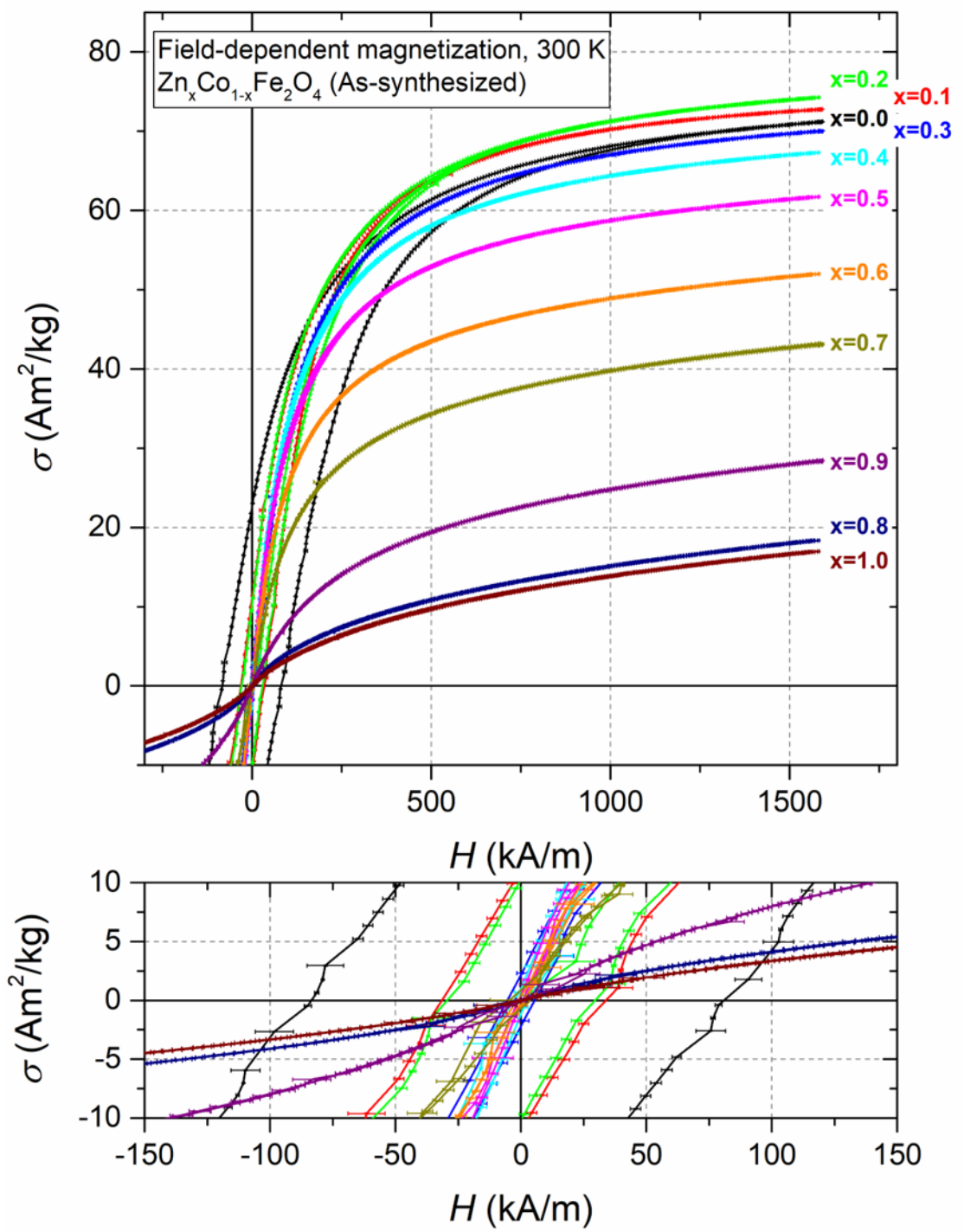

Figure S20: Room temperature field-dependent magnetization curves of the indicated as-synthesized $Zn_xCo_{1-x}Fe_2O_4$ samples and a magnification of the low H region.

Hysteresis curves (x=0.0-1.0, Annealed)

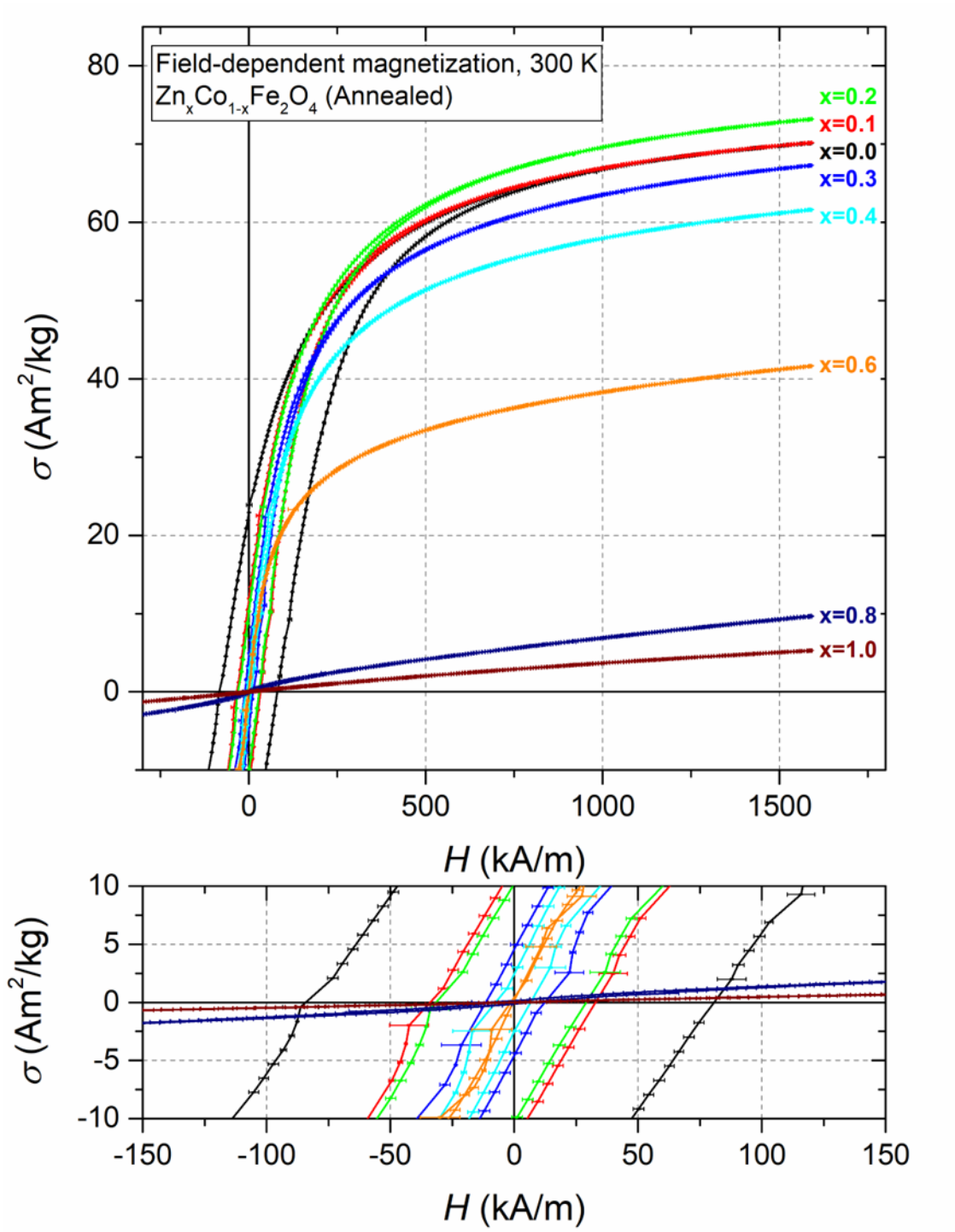

Figure S21: Room temperature field-dependent magnetization curves of the indicated annealed $Zn_xCo_{1-x}Fe_2O_4$ samples and a magnification of the low H region.

Coercive field and magnetic remanence

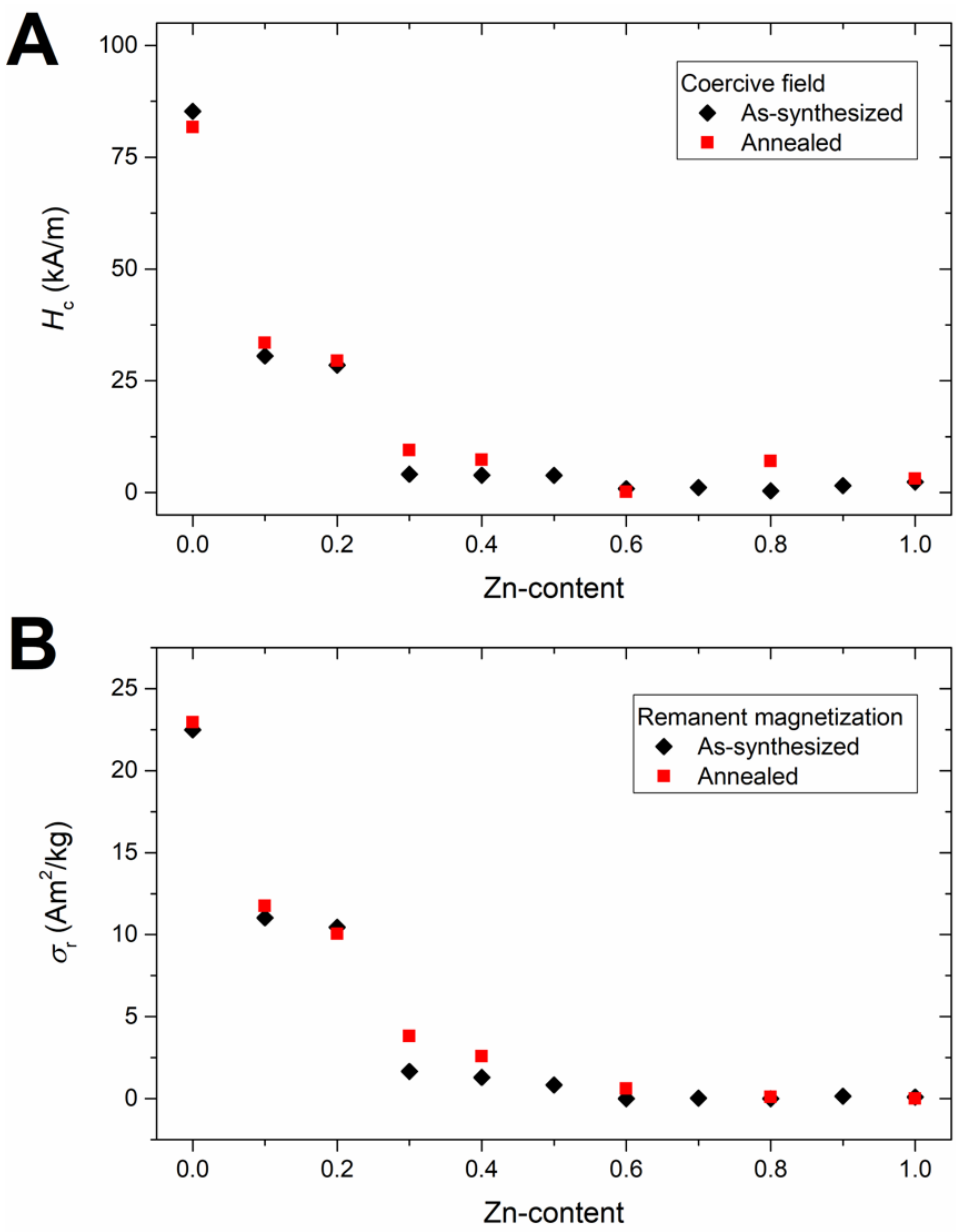

Figure S22: A) Coercive field (H_c) as function of Zn-content for as-synthesized and annealed $Zn_xCo_{1-x}Fe_2O_4$ samples. B) Remanent magnetization (σ_r) as function of Zn content for as synthesized and annealed $Zn_xCo_{1-x}Fe_2O_4$ samples.

References

1. F. Gozuak, Y. Koseoglu, A. Baykal and H. Kavas, *J. Magn. Magn. Mater.*, 2009, **321**, 2170-2177.
2. H. Sozeri, Z. Durmus and A. Baykal, *Mater. Res. Bull.*, 2012, **47**, 2442-2448.
3. R. Topkaya, A. Baykal and A. Demir, *J. Nanopart. Res.*, 2013, **15**, 1359.
4. E. Hema, A. Manikandan, P. Karthika, S. A. Antony and B. R. Venkatraman, *J Supercond Nov Magn*, 2015, **28**, 2539-2552.
5. Y. Koseoglu, A. Baykal, F. Gozuak and H. Kavas, *Polyhedron*, 2009, **28**, 2887-2892.
6. A. K. Azad, A. K. M. Zakaria, M. Y. Jewel, A. Khan, S. M. Yunus, I. Kamal, T. K. Datta and S. G. Eriksson, *Aip. Conf. Proc.*, 2015, **1660**, 090050.
7. H. Malik, A. Mahmood, K. Mahmood, M. Y. Lodhi, M. F. Warsi, I. Shakir, H. Wahab, M. Asghar and M. A. Khan, *Ceram. Int.*, 2014, **40**, 9439-9444.
8. T. Slatineanu, A. R. Iordan, V. Oancea, M. N. Palamaru, I. Dumitru, C. P. Constantin and O. F. Caltun, *Mater. Sci. Eng. B-Adv.*, 2013, **178**, 1040-1047.
9. R. S. Yadav, J. Havlica, M. Hnatko, P. Sajgalik, C. Alexander, M. Palou, E. Bartonickova, M. Bohac, F. Frajkorova, J. Masilko, M. Zmrzly, L. Kalina, M. Hajudchova and V. Enev, *J. Magn. Magn. Mater.*, 2015, **378**, 190-199.
10. V. Mameli, A. Musinu, A. Ardu, G. Ennas, D. Peddis, D. Niznansky, C. Sangregorio, C. Innocenti, N. T. K. Thanh and C. Cannas, *Nanoscale*, 2016, **8**, 10124-10137.